*Kovove Mater. 48 2010 203–210*
*DOI: 10.4149/km_2010_3_203*



# A study on wear and corrosion behaviour of thermally sprayed alumina-titania composite coatings on aluminium alloys

H. Mindivan*

*Department of Metallurgy and Material Engineering, Engineering Faculty, Ataturk University, 25240 Erzurum, Turkey*

Received 22 September 2009, received in revised form 4 December 2009, accepted 15 December 2009

**Abstract**

In this study, $Al_2O_3$-13$TiO_2$ + 10 % polytetrafluoroethylene (PTFE) powders were sprayed using both flame and plasma spray processes after a NiAl bond layer was deposited on 2024--T6 aluminium alloy substrate. The characterization of the coatings was made by microscopic examinations, thickness, surface roughness, porosity and hardness measurements and X-ray diffraction (XRD) analysis. Corrosion and wear performances of the samples were analysed by using a potentiodynamic polarization scanning (PDS) technique and a reciprocating wear tester, respectively. It was found that the flame and plasma sprayed $Al_2O_3$-13$TiO_2$ + 10 % PTFE coatings possessed about two and four times higher wear resistance than AA2024-T6 substrate, respectively. When compared to the flame sprayed $Al_2O_3$-13$TiO_2$ + 10 % PTFE coating, the plasma sprayed $Al_2O_3$-13$TiO_2$ + 10 % PTFE coating with a lower porosity showed higher hardness and better wear and corrosion resistance.

K e y w o r d s: aluminium, coating, corrosion, thermal spray, wear

## 1. Introduction

Aluminium and its alloys, with their low density and good formability, are attractive engineering materials for the automotive, aerospace, marine, chemical, and food industries due to their high strength to weight ratio as well as good resistance to degradation in many corrosive media, including atmospheric environments, fresh and salt waters, and in many chemicals and chemical solutions. When exposed to air, aluminium alloys do not oxidize progressively because a very thin oxide film forms on the surface and isolates the metal from the environment [1, 2]. Nevertheless, they also exhibit several disadvantages: low hardness, very low load bearing capacity, poor wear resistance [3–5] and localized corrosion due to pores and other defects caused by alloying elements [6]. By the application of thin coatings such as hard anodising, electroplating and physical vapour deposition, it is possible to improve the surface properties of aluminium alloys in applications where wear and corrosion resistances are required simultaneously. But these thin coatings may fail under heavy surface loading conditions owing to the easy collapse of the thin film by a deformation of aluminium alloy substrate. Therefore, it is necessary to employ a thick, hardened coating on the surface of aluminium alloys [3–5, 7].

Thermal spraying is often considered as a thick, hardened alternative coating to replace electroplating and physical vapour deposition. Alumina and their modifications with titania coatings are conventionally used hard coatings because of their high wear resistance [8–10]. But, the chemical resistance of these coatings is poor and their performances especially in terms of wear and friction under dry sliding conditions should be improved. Polymer particles such as PTFE have been used with a ceramic matrix to enhance the chemical resistance of the coatings while providing low friction and/or high wear resistance [5, 11, 12].

In this paper, the wear and corrosion behaviours of $Al_2O_3$-13$TiO_2$ + 10 % PTFE coatings fabricated by flame and plasma spray processes are investigated and compared with the wear and corrosion behaviour of AA2024-T6 aluminium alloys and thermally sprayed $Al_2O_3$-13$TiO_2$ + 10 % PTFE coatings.

* Tel.: +90 442 231 4589; fax: +90 442 236 0957; e-mail address: hmindivan@hotmail.com

Table 1. Process parameters

| Flame spray parameters | |
|---|---|
| $O_2$ pressure (MPa) | 0.04 |
| Acetylene pressure (MPa) | 0.08 |
| Powder feed rate (lb $h^{-1}$) | 20 |
| Spray distance (mm) | 100 |
| **Plasma spray parameters** | |
| Electric current (A) | 500 |
| Electric voltage (V) | 75 |
| Powder feed rate (lb $h^{-1}$) | 3 |
| Spray distance (mm) | 65 |

## 2. Experimental procedure

An AA2024-T6 aluminium alloy with a nominal composition (wt.%) of 4.1 Cu, 0.85 Si, 1.1 Mg, 0.8 Mn, 0.08 Fe, 0.02 Zn, 0.02 Ti, and the balance of Al was used as a substrate. Prior to spraying, the aluminium substrates of 10 mm thickness and 25 mm diameter were given a surface with a mean roughness ($Ra$) of approximately 5 μm by sand blasting and then coated with a NiAl bond layer in order to improve the adhesion strength between the substrate and the $Al_2O_3$--13$TiO_2$ + 10 % PTFE coating. The mixtures of 10 wt.% PTFE with alumina-titania powders (87 wt.% small $Al_2O_3$-13wt.%$TiO_2$) were sprayed over the bond layer by flame and plasma spray processes. The process parameters selected for high deposition efficiency are listed in Table 1.

The characterization of the coatings was made by microscopic examinations, thickness, roughness, porosity and hardness measurements and X-ray diffraction analysis. Microscopic examinations were conducted on the surface and cross-section of the coated samples by a scanning electron microscope, after grinding and polishing in standard manner. Porosity of the coatings was calculated by linear intercept method [13]. The thickness, the porosity and the hardness of the coatings were measured on the polished cross-sections. Hardness measurements were carried out using a Vickers indenter with a load of 500 g (an average of 10 indentations per sample). Surface roughness of the coatings was examined with a stylus profilometer (Mahr Perthometer). XRD analysis was made by a Rigaku-type diffractometer with Cu K$\alpha$ radiation.

Wear performance of the examined samples were evaluated in ambient atmospheric condition (20 ± 1 °C and 30 ± 5 % RH) by utilizing a reciprocating wear tester. Figure 1 shows the schematic view of the wear tester utilized in this work. The reciprocating wear tests were carried out for the total testing time of

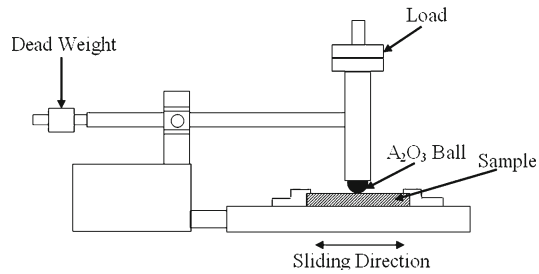


Fig. 1. Schematic view of the reciprocating wear tester utilized in this study.

125 min by applying a normal load of 1.2 N to the unlubricated surfaces of the samples with a 10 mm diameter ceramic ($Al_2O_3$) ball. During the tests, the sliding speed of the balls on the surfaces was 0.026 m $s^{-1}$ for a total sliding distance of 200 m. After the wear test, the samples were cleaned with alcohol and profiles of the wear tracks were recorded by a stylus profilometer using software version of MarSurf PS1 Explorer. Worn surfaces of the samples were surveyed on optical microscope (OM) and Jeol 5410 scanning electron microscope.

Electrochemical experiments were performed using a potentiostat/galvanostat (PCI4/750, Gamry Instruments, Inc.) in a 3.5 % NaCl aerated solution at room temperature. An Ag/AgCl and a Pt electrode were used as a reference and an auxiliary electrode, respectively. The exposed area of the samples was about 1 $cm^2$. The samples were successively ground and immersed into the solution until a steady open circuit potential (OCP) at a rate of 1 mV $s^{-1}$ was obtained. The corrosion tests were evaluated from the potentiodynamic polarization. After polarization, surfaces of the samples were ultrasonically cleaned with distilled water for surface examinations.

## 3. Results and discussion

Figure 2a–d shows the surface and cross-section of two $Al_2O_3$-13$TiO_2$ + 10 % PTFE coatings sprayed on AA2024-T6 substrates. The Ni-Al bonding layer, which was present between the aluminium substrate and the $Al_2O_3$-13$TiO_2$ + 10 % PTFE coatings, appeared in bright colour. When compared to the plasma sprayed coating, relatively coarser pores were formed in the flame sprayed coating. Quantitative metallographic studies revealed that the porosities of the flame and plasma sprayed coatings were 6 % and 2 %, respectively. In the coatings, an important PTFE loss was observed in both the flame and plasma sprayed coatings when compared with the initial PTFE/ceramic ratio. This phenomenon can be attributed to its higher viscosity at the melting state that

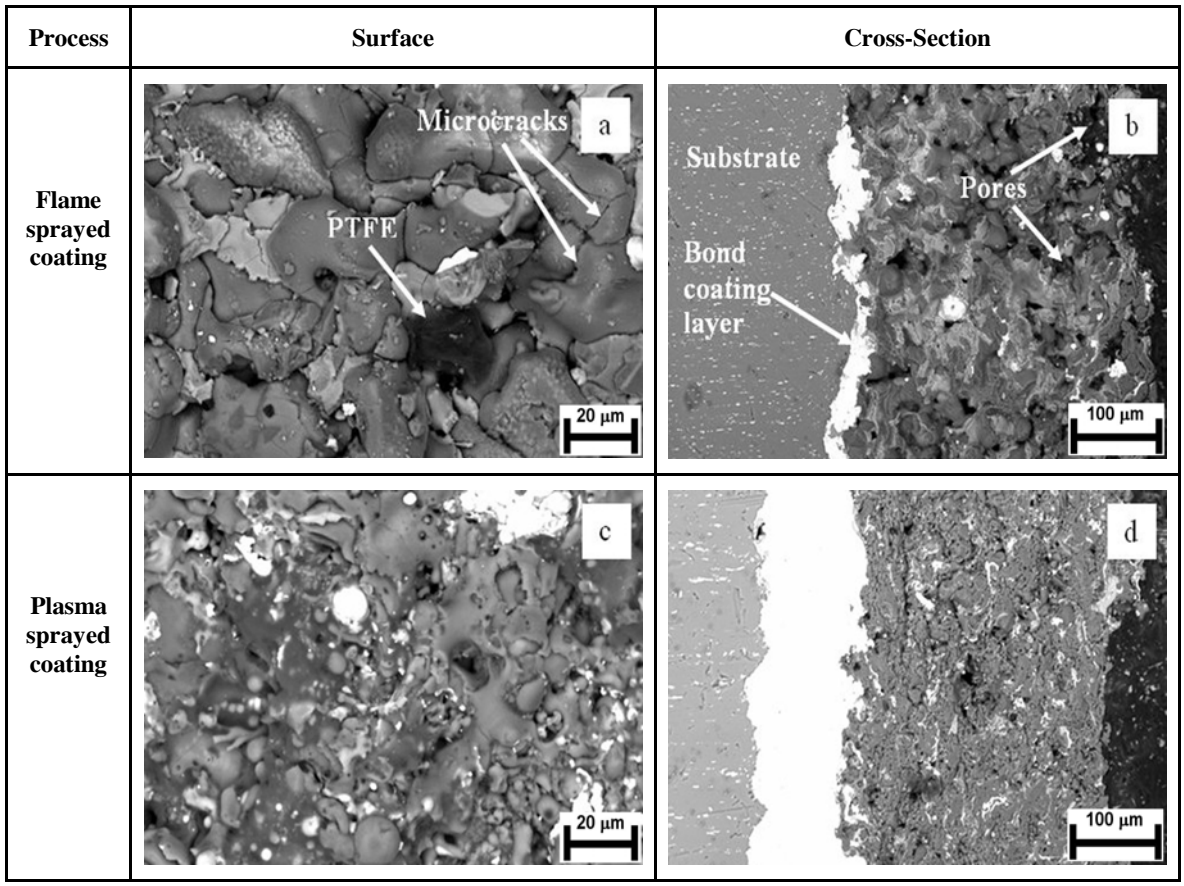


Fig. 2. Surface (a, c) and cross-section (b, d) micrographs of the coatings.

Table 2. Phases present in both the coatings

| Coating layer | Phases |
|---|---|
| Flame sprayed $Al_2O_3$-13$TiO_2$ + 10 % PTFE coating | $\alpha$-$Al_2O_3$, $TiO_2$ (rutile) |
| Plasma sprayed $Al_2O_3$-13$TiO_2$ + 10 % PTFE coating | $\alpha$-$Al_2O_3$, $\gamma$-$Al_2O_3$, $Al_2TiO_5$, $TiO_2$ (rutile) |

prevents it from flowing on the substrate surface [11]. However, no evidence of delamination or spalling has been detected along the interface of both of the coatings (Fig. 2b,d). This observation indicated that the $Al_2O_3$-13$TiO_2$ with PTFE particles cotter very well the substrate surface in both cases. It was also observed that the plasma process resulted in a quite uniform and dense coating with low porosity (2 %), indicative of good particle melting due to its higher jet temperature [14]. Since $TiO_2$ was well melted and partly mixed with alumina during the plasma spray process, white regions containing different amounts of titania were distinguished by SEM (Fig. 2d). On the other hand, the flame sprayed coating, as seen in SEM micrographs (Fig. 2a–d), included thinner bond coating layer, higher porosity content (6 %), bigger disc-shaped grains and transgranular microcracks in grains mainly induced by the "residual stress" [15] compared to the plasma sprayed coating. The thicknesses of all coatings were controlled at $\sim$ 400 μm.

XRD measurements of the coatings are summarized in Table 2. The surface layer of the flame sprayed coating mainly consisted of $\alpha$-$Al_2O_3$ and $TiO_2$ (rutile) phases (Table 2), which confirms previous results [9]. Previous studies done by Wang and Shaw [10] also showed that the presence of $\alpha$-$Al_2O_3$ in the coating could be attributed to the unmelted $\alpha$-$Al_2O_3$ inherited from the feed stock powders. The XRD analysis of the plasma sprayed coating revealed that $\alpha$-$Al_2O_3$, $\gamma$-$Al_2O_3$, $Al_2TiO_5$ and $TiO_2$ phases were present. During the plasma spray process, $\gamma$-$Al_2O_3$ phase was the predominant phase due to its minor nucleation energy, which resulted in less unmelted $\alpha$-$Al_2O_3$ in the coating. The hardnesses of the flame and plasma sprayed coatings were over 400 and 600 $HV_{0.5}$, respectively. It should be noted that these hardness values were

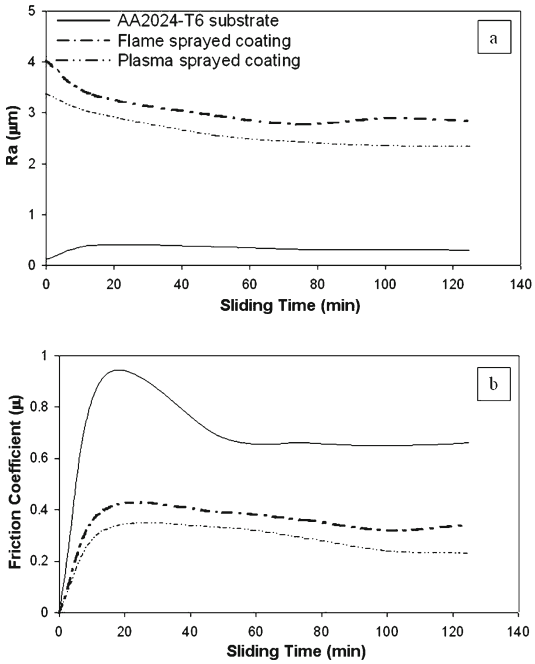


Fig. 3. Variation of (a) surface roughness and (b) average friction coefficient depending on sliding time of the coatings and AA2024-T6 substrate.

much higher than that of aluminium substrate. The observed hardness difference is believed to result partially from different phase compositions and the level of porosity [10] due to the method of spraying used, even though the initial $Al_2O_3$-13$TiO_2$/PTFE particle ratio before the coating process was the same in both the coatings. Previously, lower porosity and better performance of the plasma sprayed $Al_2O_3$-13$TiO_2$ coating were attributed to the lack of $\alpha$-$Al_2O_3$ in the coating, which was a consequence of faster cooling in plasma spraying. It is possible to claim that the plasma spray process in the coating layer provides higher density, lower $\alpha$-$Al_2O_3$ phase quantity and lower porosity content (2 %) than the flame spray process. Therefore, the lower hardness of the flame sprayed coating is likely due to the presence of a high level of porosity and a less homogeneous microstructure related to the deposition process.

The variation in the surface roughness and the average coefficient of friction with respect to the sliding time of the samples against $Al_2O_3$ ball at the same testing conditions is shown in Fig. 3a,b. The friction coefficient curves involve two-stage steps, referred to as "running in" and "steady state". The friction coefficient increases with increasing sliding time during the running in step (Fig. 3b). Since friction coefficient is very sensitive to roughness (*Ra*) of surfaces in contact [15], as presented in Fig. 3a,b, in the first step of sliding, friction coefficient was observed to increase along with a decrease in surface roughness with the increasing contact surface. At the second step, roughness and friction coefficient tend to reach some constant value (steady state) in a short time period. It can be seen

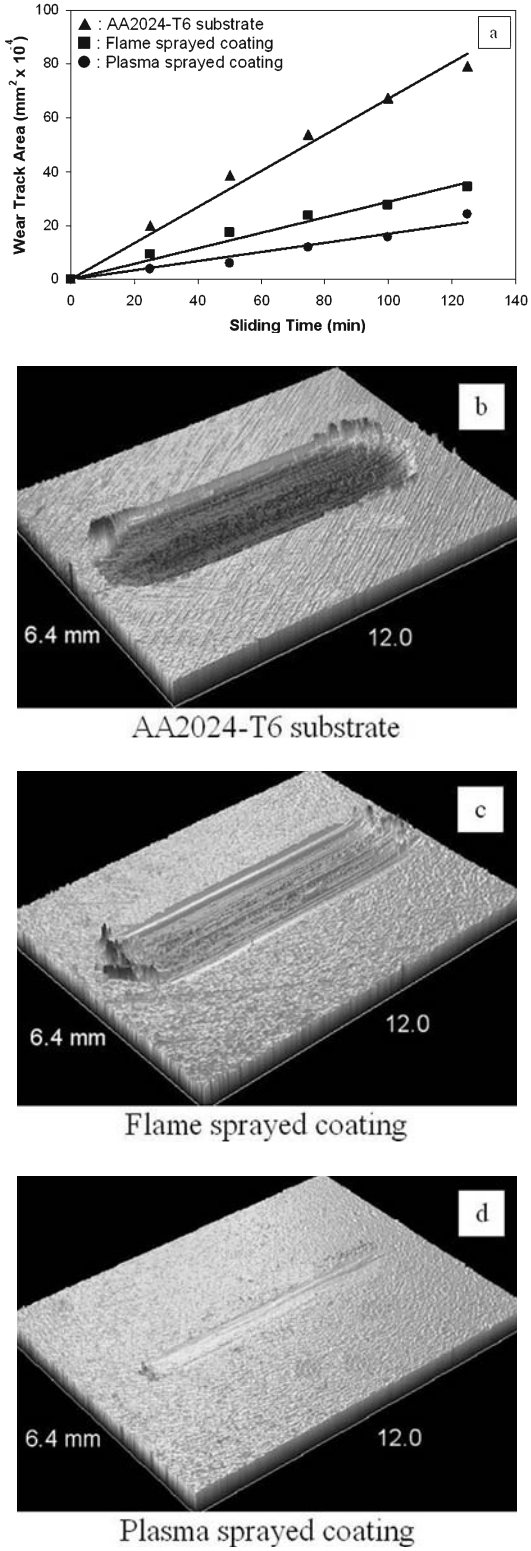


Fig. 4a–d. The wear results of the coatings and AA2024-T6 substrate.

Table 3. Wear rates and RWR values of the coatings and AA2024-T6 substrate examined

| Specimen | Wear rate ($mm^2\ min^{-1}$) | Relative wear resistance, RWR |
|---|---|---|
| AA2024-T6 substrate | $67.3 \times 10^{-2}$ | 1.0 |
| Flame sprayed $Al_2O_3$-13$TiO_2$ + 10 % PTFE coating | $28.9 \times 10^{-2}$ | 2.3 |
| Plasma sprayed $Al_2O_3$-13$TiO_2$ + 10 % PTFE coating | $16.9 \times 10^{-2}$ | 4.0 |

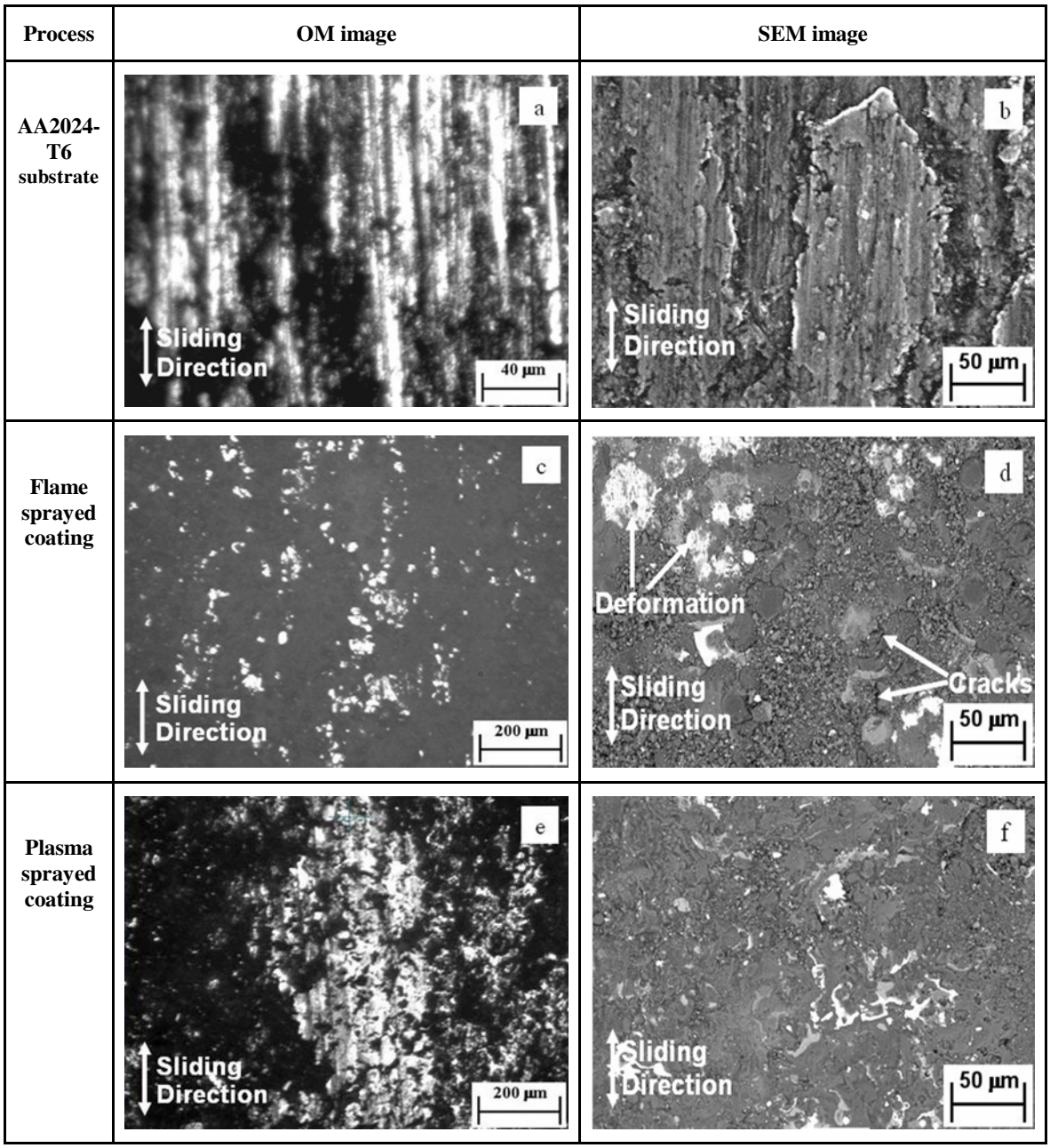


Fig. 5a–f. OM and SEM images of the wear tracks formed on the coatings and AA2024-T6 substrate.

that the roughness and the steady state friction coefficient of the plasma sprayed coating were lower than those of the flame sprayed coating in the whole testing period.

Wear track areas measured from the 3-D profiles of the wear tracks of the examined samples during the wear test are given in Fig. 4a as a function of sliding time. When compared to the flame and plasma

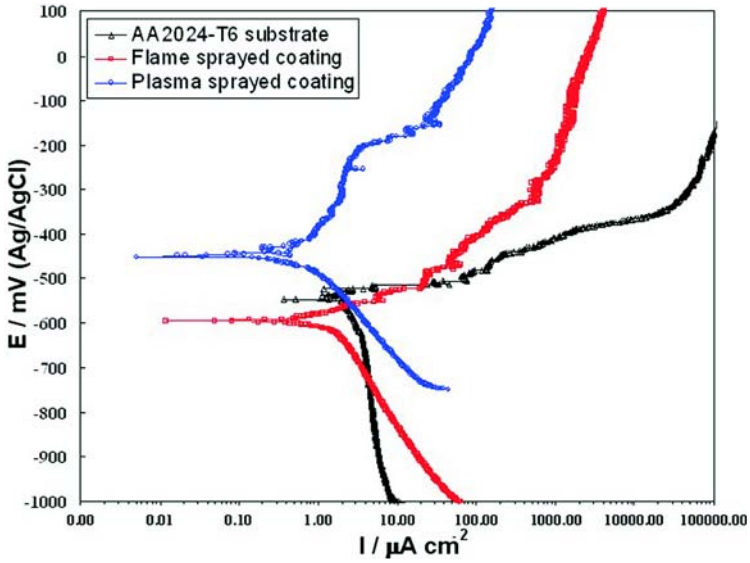


Fig. 6. Potentiodynamic polarization curves of the coatings and AA2024-T6 substrate.

sprayed coatings, considerably larger wear track areas were developed on AA2024-T6 substrate (Fig. 4b–d). The wear track area of the samples under the normal load of 1.2 N increased linearly with increasing sliding time. The slope of Fig. 4a defines the wear track area per unit sliding time in unit of $mm^2\,min^{-1}$ and is known as wear rate. The results of the wear tests were quantified in terms of wear rate and relative wear resistance (RWR) in Table 3. AA2024-T6 substrate was taken as the reference sample because it had the largest wear rate, and RWR was calculated by dividing the wear rate of AA2024-T6 substrate by that of each coating. It was shown that the wear resistances of flame and plasma sprayed coatings were about two and four times higher than that of AA2024-T6 substrate, respectively.

OM and SEM images of the wear tracks developed on the surfaces of the examined samples during wear tests are presented in Fig. 5a–f. When compared to the flame and plasma sprayed coatings, AA2024-T6 substrate underwent a large plastic deformation and exhibited a rough wear surface as shown in Fig. 5a–f. OM examinations disclosed the presence of ridges and grooves aligned parallel to the sliding direction (Fig. 5a), but the rough worn surface with irregular layers appeared in the SEM image (Fig. 5b). Although severe plastic deformation along with grooves parallel to the sliding direction were clearly evident on the OM micrograph of the wear track of the plasma sprayed coating (Fig. 5e), a very smooth worn surface (without significant evidence of plastic deformation) was noticed during SEM examinations (Fig. 5f). By OM examinations, discontinuous wear tracks were observed inside the wear track of the flame sprayed coating (Fig. 5c), which indicated that the degree of plastic deformation of the flame sprayed coating was lower than that of the plasma sprayed coating. The presence of transgranular microcracks on the surface of the coating applied by flame spray process was previously stated (Fig. 2a). SEM examinations showed that these grains were cracked with applied load and extended in the sliding direction during sliding period of $Al_2O_3$ ball (Fig. 5d). Also, randomly distributed cracks were observed inside the wear track of the flame sprayed coating, when compared with the plasma sprayed coating. Chen et al. [16] declared that the wear resistance was improved by both the enhanced cohesion properties of the coating as it increased the contact points between splats due to the good melting of feedstock powders in the plasma jet and the occurrence of plastic deformation associated with the decrease of porosity in the coating. Therefore, the low roughness and friction coefficient (Fig. 3a,b) along with improved wear resistance (Table 3) and hardness of the plasma sprayed coating is possibly due to a good cohesion between splats and a lower porosity in the coating, which improved the ability of plastic deformation.

Figure 6 shows the typical PDS curves for AA2024-T6 substrate, the flame sprayed $Al_2O_3$-13$TiO_2$ + 10 % PTFE coating with an average porosity of 6 % and the plasma sprayed $Al_2O_3$-13$TiO_2$ + 10 % PTFE coating with an average porosity of 2 %. The plasma sprayed coating with low porosity showed the highest corrosion potential ($E_{corr}$), which implied a delay in the electrolyte penetration. This behaviour can be associated with the existence of a more dense structure in the plasma sprayed coating (Fig. 2c,d). However, the presence of porosity and cracks in the flame sprayed coating was able to allow a higher velocity of electrolyte penetration through the coating, which promoted the attack of the aluminium substrate. This

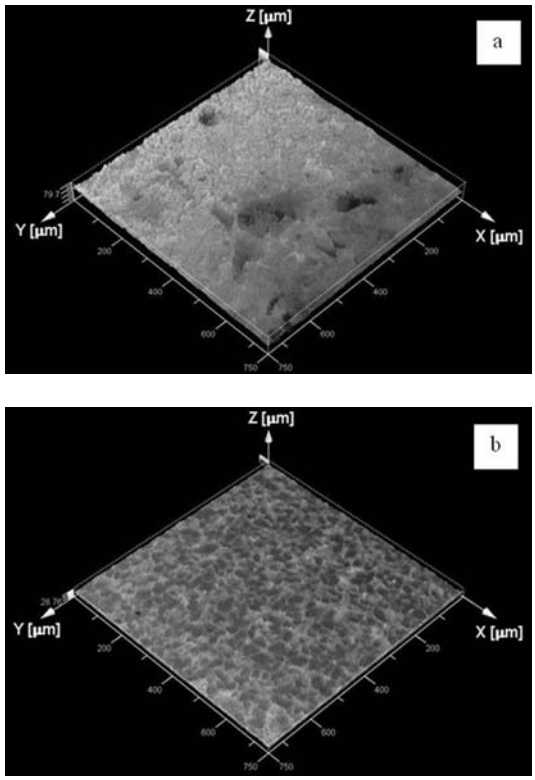


Fig. 7. Surface topographies of the (a) flame and (b) plasma sprayed coatings after corrosion tests.

result is consistent with the findings of Aw et al. [17] and Khaled et al. [18], who reported the improvement in corrosion resistance with decrease in porosity and cracks in the coating. The plasma sprayed coating with the most positive $E_{corr}$ (–450 mV) and the lowest corrosion current intensity (0.314 µA cm$^{-2}$) suffered the least corrosion attack that provided a good protection for the aluminium substrate against corrosion. In general, extensive deterioration with regard to surface appearance after corrosion tests had taken place on the surface of the flame sprayed coating (Fig. 7a), while it was much less pronounced on the surface of the plasma sprayed coating (Fig. 7b). The PDS curves (Fig. 6) showed a good level of consistency with the microscopic observations (Fig. 7a,b).

## 4. Conclusions

$Al_2O_3$-13$TiO_2$ + 10 % PTFE powders with the same chemical composition were sprayed onto an AA2024-T6 aluminium alloy by flame and plasma spray processes and the following conclusions were reached:

1. $Al_2O_3$-13$TiO_2$ + 10 % PTFE coating performed by the plasma spray process improved the wear resistance of AA2024-T6 substrate four times while the flame sprayed $Al_2O_3$-13$TiO_2$ + 10 % PTFE coating improved the wear resistance of AA2024-T6 substrate twice.

2. Compared with the flame spray process, the plasma spray process provided higher hardness and better wear and corrosion resistances. The improved wear and corrosion resistances of the plasma sprayed $Al_2O_3$-13$TiO_2$ + 10 % PTFE coating can be attributed to a more dense structure with low porosity and enhanced cohesion of the coating, which improved the ability of plastic deformation.

## Acknowledgements

The author would like to thank Senkron Metal & Ceramic Coating Company of Turkey for performing plasma and HVOF spraying. The author is also grateful to Dr. Ramazan SAMUR for his assistance during the study.

## References

[1] MONDOLFO, L. F.: Aluminum Alloys: Structure and Properties. Boston, Butterworths 1976.
[2] ROOY, E. L.: Properties and Selection: Nonferrous Alloys and Special-Purpose Materials. Metals Park, OH, ASM International 1994.
[3] GADOW, R.—SCHERER, D.: Surf. Coat. Technol., *151–152*, 2002, p. 471.
[4] WENZELBURGER, M.—ESCRIBANO, M.—GADOW, R.: Surf. Coat. Technol., *180*, 2004, p. 429.
[5] AKIN, U.—MINDIVAN, H.—SAMUR, R.—KAYALI, E. S.—CIMENOGLU, H.: Key Eng. Mater., *280–283*, 2005, p. 1453.
[6] PALOUMPA, I.—YFANTIS, A.—HOFFMANN, P.—BURKOV, Y.—YFANTIS, D.—SCHMEIßER, D.: Surf. Coat. Technol., *180–181*, 2004, p. 308.
[7] GIBBONS, G. J.—HANSELL, R. G.: J. Mater. Process. Technol., *204*, 2008, p. 184. doi:10.1016/j.jmatprotec.2007.11.032
[8] BOLELLI, G.—CANNILLO, V.—LUSVARGHI, L.—MANFREDINI, T.: Wear, *261*, 2006, p. 1298.
[9] HABIB, K. A.—SAURA, J. J.—FERRER, C.—DAMRA, M. S.—GIMÉNEZ, E.—CABEDO, L.: Surf. Coat. Technol., *201*, 2006, p. 1436. doi:10.1016/j.surfcoat.2006.02.011
[10] WANG, M.—SHAW, L. L.: Surf. Coat. Technol., *202*, 2007, p. 34.
[11] MATEUS, C.—COSTIL, S.—BOLOT, R.—CODDET, C.: Surf. Coat. Technol., *191*, 2005, p. 108.
[12] WANG, Y.—LIM, S.: Wear, *262*, 2007, p. 1097.
[13] VANDER VOORT, G. F.: Metallography Principles and Practice. New York, McGraw-Hill Book 1999.
[14] PÁLKA, V.—POŠTRKOVÁ, E.—KOLENČIAK, V.: Kovove Mater., *34*, 1996, p. 367.
[15] KUSOGLU, I. M.—CELIK, E.—CETINEL, H.—OZDEMIR, I.—DEMIRKURT, O.—ONEL, K.: Surf. Coat. Technol., *200*, 2005, p. 1173. doi:10.1016/j.surfcoat.2005.02.219
[16] CHEN, H.—ZHANG, Y.—DING, C.: Wear, *253*, 2002, p. 885.

[17] AW, P. K.—TAN, A. L. K.—TAN, T. P.—QIU, J.: Thin Solid Films, *516*, 2008, p. 5710. doi:10.1016/j.tsf.2007.07.065

[18] KHALED, M. M.—YILBAS, B. S.: Surf. Coat. Technol., *202*, 2007, p. 433. doi:10.1016/j.surfcoat.2007.06.011